

A Space Communications Study

Progress Report

September 15, 1967 - March 15, 1968

Prepared for

ional Aeronautics & Space Administration

Electronic Research Center

under

NASA GRANT NGR - 33-006-020

GPO PRICE \$
CFSTI PRICE(S) \$
Hard copy (HC) 3.00
Microfiche (MF) 60

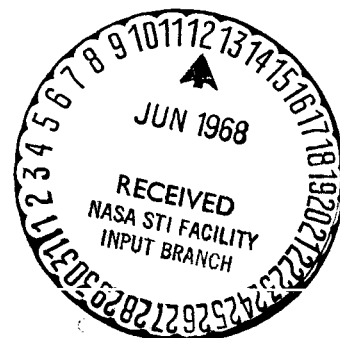
ff 653 July 65

FACILITY FORM 602

498-25366
(ACCESSION NUMBER) (THRU)
53 (PAGES)
Lit # 94775 (NASA CR OR TMX OR AD NUMBER)
(CODE) 07
(CATEGORY)

DEPARTMENT OF ELECTRICAL ENGINEERING
POLYTECHNIC INSTITUTE OF BROOKLYN

RECEIVED
JUN 10 3 50 PM '68
OFFICE OF
UNIVERSITY AFFAIRS



A Space Communications Study

Progress Report

September 15, 1967 - March 15, 1968

Prepared for

National Aeronautics & Space Administration

Electronic Research Center

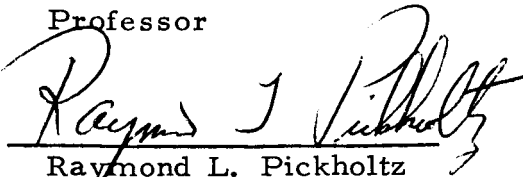
under

NASA GRANT NGR - 33-006-020

PRINCIPAL INVESTIGATORS:



Kenneth K. Clarke
Professor



Raymond L. Pickholtz
Associate Professor



Donald L. Schilling
Associate Professor

DEPARTMENT OF ELECTRICAL ENGINEERING
POLYTECHNIC INSTITUTE OF BROOKLYN

Introduction

This progress report summarizes some of the research conducted from 15 September 1967 to 15 March 1968.

During this period, the following problems were considered :

1. Optimum Estimation
2. Solution of the 1st, 2nd, and 3rd order Phase Locked Loop Equations
3. Threshold Extension of the Frequency Locked Loop
4. Spike Detection and Correction
5. Thresholds in FM/FM Systems
6. Threshold of SSB/FM Systems
7. Synchronization of PSK Signals
8. Transmission & Reception of Television Signals through a Noisy Channel
9. A study of a Slow-Scan TV
10. Data Compression Techniques with Application to TV
11. Extreme-Value Detection: A New Non Parametric Detector
12. FM Multipath
13. Recursive Techniques

Three of these projects are discussed below. A complete report summarizing all of the research conducted under this grant will be presented in September 1968. In that final report, a complete list of papers published, Ph.D. dissertations, and Masters Theses, will also be given.

Contributors to this report are: Professors Boorstyn, Clarke, Hess, Pickholtz, Schilling, and Wolf; also Messrs. Cassara, Hoffman, Milstein, Oberst, Osborne, Stochel, Tepedelenlioglu, Unkauf and Zeger.

I. THRESHOLD PERFORMANCE OF PHASE LOCKED LOOP DEMODULATORS

A new method is presented for finding the expected number of spikes in a phase locked loop of any order, with or without modulation. The procedure can also be employed to determine the threshold of FMFB, FM discriminators and the Maximum likelihood Estimator. The low pass equivalent gaussian noises $x(t)$, $y(t)$ in the differential equation describing the system (PLL or FMFB) are replaced by the deterministic time functions (Conditional Expectations)

$$1) \quad E[x(t) | x(o), \dot{x}(o)]$$

$$2) \quad E[y(t) | y(o), \dot{y}(o)]$$

and solved on a digital computer. The mid spike time ($t = 0$) is taken to be the time when $x(o)$ (quadrature noise) = 0, and a surface (s) in $\dot{x}(o)$, $y(o)$, $\dot{y}(o)$ space is determined which indicates the region A where spikes in the demodulator are obtained. From this the expected number of spikes per second is calculated.

Results are presented for the first and the second order (using a constant plus integral filter) phase locked loop, and for an ordinary FM discriminator (which can be shown to be equivalent to a PLL of infinite gain).

Introduction

For the past several years there has been a great deal of research to determine the threshold behavior of the phase locked loop.⁽¹⁾ However, there are important deficiencies in the analyses to date. These analyses have assumed that the input noise is white, and have neglected the effect of the modulation. The design of a PLL is, however, vastly different if there is modulation than when there is no modulation.

The expected number of spikes in the output of a phase locked loop decreases as the gain of the PLL is reduced, if there is no modulation. When modulation is present, one finds that there is a minimum loop bandwidth below which distortion results. The spikes present in this region is large. Increasing the PLL bandwidth results in a decrease in the number of spikes. However, we know that infinite bandwidth is equivalent to using a discriminator, hence an optimum bandwidth exists which can only be found by considering the effect of the modulation.

In this paper a Carson's rule 3dB IF bandwidth equal to $2(\beta + 1) f_m$ Hz is employed, where β is the modulation index, and f_m the modulation frequency. Square wave modulation is considered. The square wave modulation represents a worst-case solution since the number of spikes occurring per second is proportional to the deviation Δf ⁽²⁾.

Mathematical Preliminaries

A. FM Discriminator

The output of an FM discriminator when integrated is :

$$v_{\text{FMD}}(t) = \phi_M(t) + \arctan \left(\frac{x(t) \cos \phi_M + y(t) \sin \phi_M}{1 + x(t) \sin \phi_M - y(t) \cos \phi_M} \right) \quad (1.1)$$

where

ϕ_M = phase of the modulating signal

$x(t)$ = quadrature low pass equivalent noise

$y(t)$ = in phase low pass equivalent noise

A spike occurs when the arctan term jumps $\pm 2\pi$ (see Ref. 2).

B. Phase Locked Loop Differential Equations

1. First Order Loop

A block diagram of a first order phase locked loop is shown in Figure 1.

The differential equation describing the loop is easily shown to be

$$\dot{\phi} + G \sin(\phi - \phi_M) = G(x(t) \cos \phi + y(t) \sin \phi) \quad (1.2)$$

where

ϕ = phase of VCO output

G = loop gain and 3dB bandwidth of PLL.

We let the modulating signal be $2\pi \Delta f$. Thus $\phi_M(t) = 2\pi(\Delta f)t$. When considering noise, this represents a worst case solution.

The solution of Eq. 2 with no noise is

$$\phi(t) = 2\pi t\Delta f - \arcsin\left(\frac{2\pi\Delta f}{G}\right) \quad (1.3)$$

For proper operation of the PLL (low distortion) the error voltage $(\phi - \phi_M)$ must be much smaller in magnitude than $\pi/2$, or

$$\arcsin\left(\frac{2\pi\Delta f}{G}\right) \ll \frac{\pi}{2} \quad (1.4)$$

which implies that

$$G \gg 2\pi \Delta f \quad (1.5)$$

2. Second Order Loop

A block diagram of a second order constant plus integral phase locked loop is shown in Fig. 2. The differential equation describing the loop is:

$$\begin{aligned} \ddot{\phi} + 2G_1 [x(t) \sin \phi - y(t) \cos \phi + \cos(\phi - \phi_M)] \\ \phi + G_1 G_2 \sin(\phi - \phi_M) = G_1 [(2\dot{x} + G_2 x) \cos \phi + \\ + (2\dot{y} + G_2 y) \sin \phi + \dot{\phi}_M \cos(\phi - \phi_M)] \end{aligned} \quad (1.6)$$

where

ϕ is the phase of the VCO output

$G_1(2 + G_2)/s$ - is the transfer function of the constant plus integral filter.

When there is no noise and $|\phi - \phi_M| \ll \frac{\pi}{2}$, and the PLL equation becomes,

$$\ddot{\phi} + 2G_1 \dot{\phi} + G_1 G_2 \phi = G_1 G_2 \phi_M + G_1 \dot{\phi}_M \quad (1.7)$$

and

$$\Phi(p) = \frac{2G_1 p + G_1 G_2}{p^2 + 2G_1 p + G_1 G_2} \Phi_M(p) \quad (1.8)$$

In this report $G_1 = G_2 = G$ (critically damped). Equation 1.8 reduces to

$$\Phi(p) = \frac{2G(p + G/2)}{(p + G)^2} \Phi_M(p) \quad (1.9)$$

The 3db bandwidth of the PLL is $\sqrt{\sqrt{10} + 3}G \approx 2.5G$.

The better way to view this loop is to consider the transfer between the modulating phase and the error phase of the loop, since for proper operation, this error phase must be much less than $\frac{\pi}{2}$. Then

$$\Phi_e(p) = \Phi(p) - \Phi_M(p) = \frac{p^2}{(p \pm G)^2} \Phi_M(p) \quad (1.10)$$

This represents a high pass filter with a 3db lower frequency of

$\sqrt{\sqrt{2} - 1}G \approx 0.645G$. For proper operation, the modulating frequencies must be considerably less than $0.643G$ in order to maintain a small phase (for low distortion). Thus, the error bandwidth $0.643G$ is of more practical interest than the PLL bandwidth. For example, if $\phi_M(t) = \beta \sin \omega_m t$

$$\phi_e(t) = \frac{\beta \omega_m^2}{\omega_m^2 + G^2} \sin \left[\omega_m t - \arctan \left(\frac{2\omega_m G}{G^2 - \omega_m^2} \right) \right] \quad (1.11)$$

From Eq. 1.11, for low distortion, G must be such that

$$\frac{\beta \omega_m^2}{\omega_m^2 + G^2} \ll \frac{\pi}{2} \quad (1.12)$$

C. Noise Model

Instead of the random processes $x(t)$ and $y(t)$, which are the quadrature and in phase low pass equivalent noises respectively, we shall use the following deterministic signals (conditional expectations) with random variable parameters :

$$x_1(t) = E(x(t) / x(0), \dot{x}(0)) \quad (1.13)$$

$$y_1(t) = E(y(t) / y(0), \dot{y}(0)) \quad (1.14)$$

We consider the mid spike time, $t = 0$, as being the time when $x(0) = 0$. Thus, Eq. 1.13 becomes

$$x_1(t) = E(x(t) / x(0) = 0, \dot{x}(0)) \quad (1.15)$$

The IF filter is assumed to consist of the cascade of two identical stages, each single tuned with a 3db bandwidth of two radians per second. Thus, the low pass noise components $x(t)$ and $y(t)$ have the spectrum

$$S(\omega) = \frac{4\sigma^2}{(\omega^2 + 1)^2} \quad (1.16)$$

where σ^2 is the variance of the random processes $x(t)$, $y(t)$. It then follows that:

$$R(t) = R_x(t) = R_y(t) = \frac{1}{2\pi} \int_{-\infty}^{\infty} S(\omega) e^{j\omega t} d\omega = \sigma^2 (1 + |t|) e^{-|t|} \quad (1.17a)$$

$$R_{\dot{x}\dot{x}}(t) = R_{\dot{y}\dot{y}} = \frac{1}{2\pi} \int_{-\infty}^{\infty} (-j\omega) S(\omega) e^{j\omega t} d\omega = -\dot{R}(t) = \sigma^2 t e^{-|t|} \quad (1.17b)$$

The conditional density of $x(t)$ given $x(o)$, $\dot{x}(o)$ is

$$f(x(t)/x(o), \dot{x}(o)) = \frac{e^{-\left(x(t) - x(o)\frac{R(t)}{\sigma^2} + \dot{x}(o)\frac{\dot{R}(t)}{\sigma^2}\right)^2} 2\sigma^2 \left(1 - \frac{R^2(t)}{\sigma^4} - \frac{\dot{R}^2(t)}{\sigma^4}\right)}{\sqrt{2\pi\sigma^2 \left(1 - \frac{R^2(t)}{\sigma^4} - \frac{\dot{R}^2(t)}{\sigma^4}\right)}} \quad (1.18)$$

The conditional density of $y(t)$, $f(y(t) / y(o), \dot{y}(o))$ has the same form as

Eq. 1.19

Using Eqs. 1.17a, 1.17b, and 1.18, we find for the following conditional expectations :

$$x_1(t) = E[x(t) / x(o) = 0, \dot{x}(o)] = \dot{x}(o) t e^{-(t)} \quad (1.19a)$$

$$y_1(t) = E[y(t) / y(o), \dot{y}(o)] = \{y(o) (1 + (t)) + \dot{y}(o) t\} e^{-(t)} \quad (1.19b)$$

The above deterministic functions is the noise model used in the PLL analyses which follows. A typical noise trajectory is shown in Fig. 3.

D. Computation of the Expected Number of Spikes per Second

Using a digital computer, and the noise model of Eq. 1.19, the differential equations of the PLL (see Eq. 1.2 and Eq. 1.6) are solved. A fourth order Runge-Kutta starting procedure is used, with a Moultons predictor-corrector program. The solution is made over a period of time from

$\dot{t} = -5$ to $t = +12$ seconds. A hunting procedure on the parameters $\dot{x}(o)$, $y(o)$, $\dot{y}(o)$ is used in the program such that a "spike" surface in $\dot{x}(o)$, $y(o)$, $\dot{y}(o)$ space is determined. Values of the parameters $\dot{x}(o)$, $y(o)$, $\dot{y}(o)$ on one side of this surface cause the phase error between the phase output of the PLL VCO, and the phase of the modulation to be $\pm \pi$ at $t = 12$ seconds. Values of the parameters on the other side of this surface are zero when $t = 12$ seconds.

The expected number of spikes per second is simply the expected number of times the random vector $\dot{x}(o)$, $y(o)$, $\dot{y}(o)$ is in a spike region. From Rice⁽²⁾, we get

$$N = \int_S |\dot{x}| f(x(o) = 0, \dot{x}(o), y(o), \dot{y}(o)) d\dot{x} dy d\dot{y} \quad (1.20)$$

where S = spike regions

N = expected number of spikes/sec

$f(x, \dot{x}, y, \dot{y})$ = joint gaussian density of x, \dot{x}, y, \dot{y}

The integral is performed by approximating the spike surfaces by plane segments, and summing the results of Eq. 1.20 for each segment. A digital computer was used to perform this tedious computation.

To simplify computations, the equations were normalized. The 3db bandwidth of the IF filter is

$$\omega'_{IF} = 2(0.643) = 1.286 \text{ radians/sec.} \quad (1.21)$$

To compare the results for this IF bandwidth to results for other bandwidths we may introduce a time scale to the phase lock loop equations :

$$t' = t/K \quad (1.22a)$$

This results in a new IF frequency :

$$\omega_{IF} = K \omega'_{IF} \text{ radians/sec.} \quad (1.22b)$$

for the first order loop,

$$G = KG = \frac{\omega_{IF}}{\omega'_{IF}} G' \quad (1.23)$$

while for the second order loop

$$G_1 = \frac{\omega_{IF}}{\omega'_{IF}} G'_1 \quad (1.24a)$$

$$G_2 = \frac{\omega_{IF}}{\omega'_{IF}} G'_2 \quad (1.24b)$$

The number of spikes /second is then

$$N = KN = \frac{\omega_{IF}}{\omega'_{IF}} N' \quad (1.25a)$$

or

$$N' = \frac{\omega'_{IF}}{\omega_{IF}} N = \frac{\sqrt{\sqrt{2}-1}}{\omega_{IF}/2} N \quad (1.25b)$$

where

β = modulation index

f_m = modulating frequency

ω_{IF} = IF bandwidth (radians/sec).

2. Results :

The spike boundary can be found for the FM discriminator by plotting Eq. 1.1 from $t = 5$ to $+ 12$ seconds instead of solving a differential equation. Fig. 4 shows the resulting spike surface for a FM discriminator with a constant modulation offset of 0.6 radians/second. (This is equivalent to square wave modulation). It is interesting to note that there are multiple spike regions and that no positive spikes occur in the regions shown.

The surface for the first order PLL with no modulation is shown in Fig. 5. Negative spikes occur for values of $\dot{x}(o)$, $y(o)$, $\dot{y}(o)$ to the right of the surface and none for those to the left. The surface for positive spikes is simply a mirror image of the one shown, below the $y(o)$, $y(o)$, plane. When we have the same kind of modulation that was described above for the FM discriminator we obtain the surface shown in Fig. 6. Again, the spike region is to the right (negative spikes). The surface is shown only for position $\dot{y}(o)$ because the surface is symmetrical in $\dot{y}(o)$

For the second order, critically damped PLL with a proportional plus integral filter, a sine wave modulation was used, in order to determine where most spikes occur. It was found that they occurred almost always when the peak frequency deviation occurred. Since the bandwidth of the PLL is considerably broader than the modulating frequency, to consider the probability of receiving spikes at the peak of the sine wave modulation is

practically equivalent to considering the probability of receiving spikes with a constant input frequency deviation. ($\simeq 0.6$ radians/sec.). The resulting spike surface is shown in Fig. 7.

The expected number of spikes per second for the above surfaces was calculated using Eq. 1.20. The normalized results are plotted in Fig. 8. The curves for the first order PLL show that spikes are approximately a thousand times more frequent with modulation than without. Also it is evident that the second order PLL with modulation is almost a hundred times better than the first order with modulation.

Conclusions

The expected number of spikes, for an FM Discriminator with modulation, obtained from the spike surface of Fig. 4, was found to be almost the same as that for no modulation. These results, together with a simple approach heuristically derived by Rice⁽²⁾, are compared in Fig. 8. The difference, in terms of carrier to noise ratio, is only 0.5 db.

It is worth noting that the method allows the comparison of different systems by comparing their respective spike boundary surfaces. If the surface of one system is closer to the origin than another, then the first system generated more spikes than the second under the same conditions.

The present work on PLL systems is being extended to higher order loops and work on FMFB has begun.

References

1. A.J. Viterbi, "Phase Locked Loop Dynamics in the Presence of Noise by Fokker Planck Techniques" Proc. IEEE - December, 1963, Vol. 51, No. 12, pp. 1737-1753.

V.I. Tikhonov, "The Effects of Noise on Phase Lock Oscillation Operations," Auto-matika Telemekhanika, Vol. 22, No. 9, 1959.

R.C. Tausworthe, "A Method for Calculating Phase Locked Loop Performance Near Threshold," IEEE Transactions on Communication Theory Technology, August, 1967.

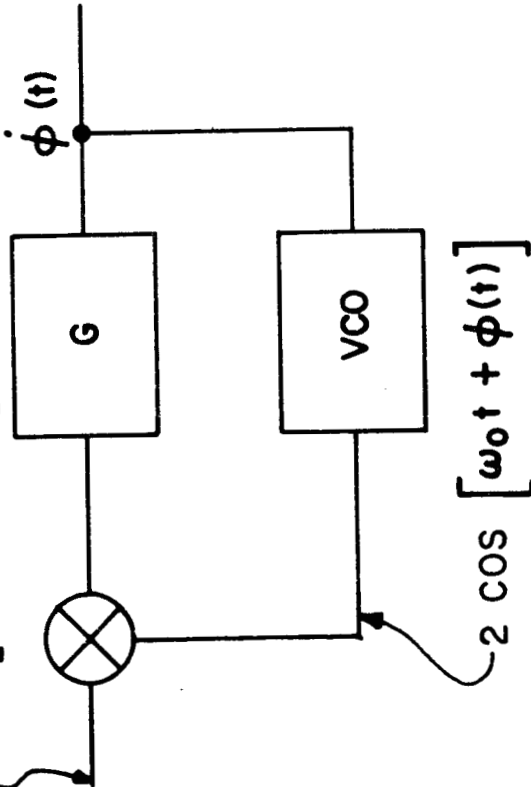
2. S.O. Rice, "Noise in FM Receivers," Time Series Analysis, Ch. 25, Wiley, 1963.

Schilling, Nelson and Hoffman, "Error Rates for Digital Signals Demodulated by an FM Discriminator," IEEE Transactions on Communication Technology, August, 1967.

3. This method was suggested in a private correspondence with S.O. Rice of the Bell Telephone Laboratories.

FIRST ORDER PLL

$$\sin [\omega_0 t + \phi_m(t)] + x(t) \cos(\omega_0 t) - y(t) \sin(\omega_0 t)$$



3 dB BANDWIDTH
= G RADIANS / SEC.

LOW PASS EQUIVALENT
NOISES

$x(t)$ - QUADRATURE

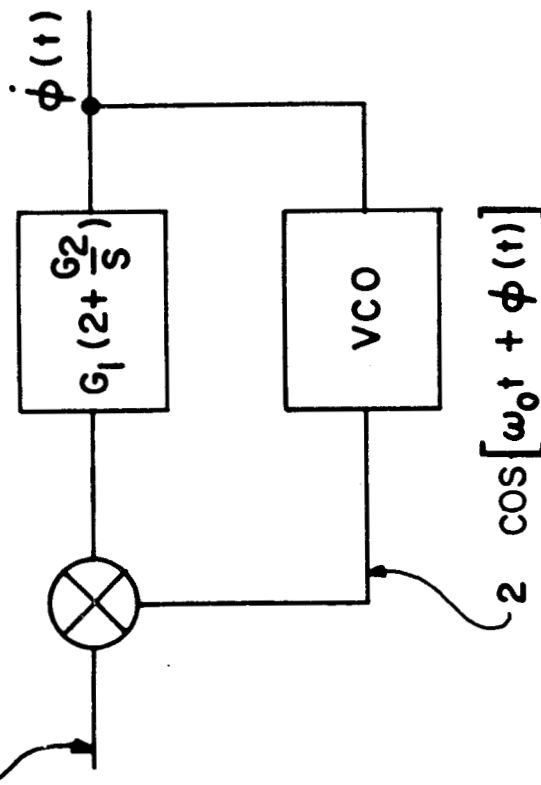
$y(t)$ - IN PHASE

$$2 \cos [\omega_0 t + \phi(t)]$$

FIG 1

SECOND ORDER PLL (CONSTANT PLUS INTEGRAL)

$$\sin[\omega_0 t + \phi_m(t)] + x(t) \cos(\omega_0 t) - y(t) \sin(\omega_0 t)$$



CRITICALLY DAMPED
WHEN $G_1 = G_2 = G$

6dB BANDWIDTH
 $= G$ RAD/SEC

LOW PASS EQUIVALENT
NOISES

$x(t)$ - QUADRATURE

$y(t)$ - IN PHASE

FIG 2

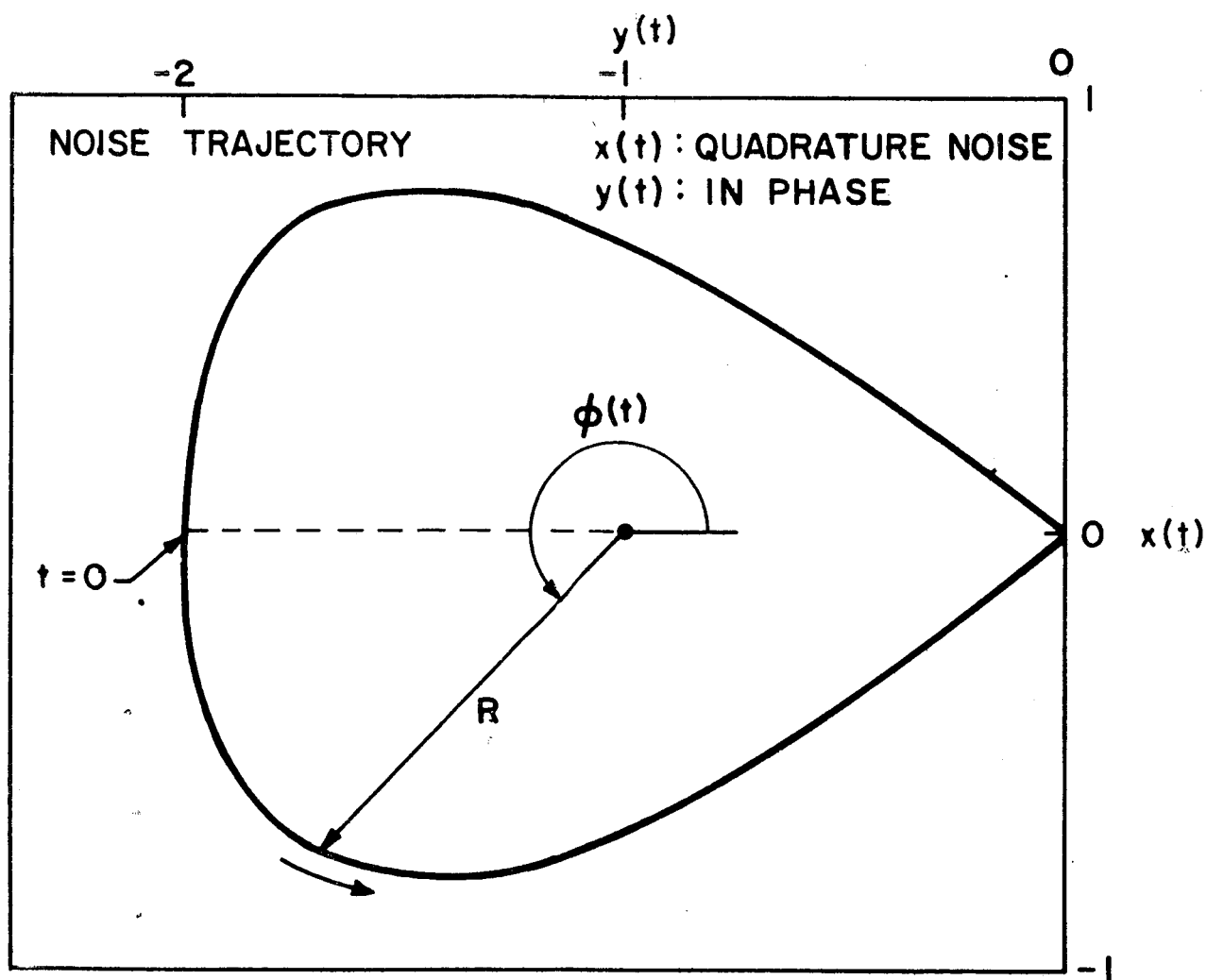


FIG. 3

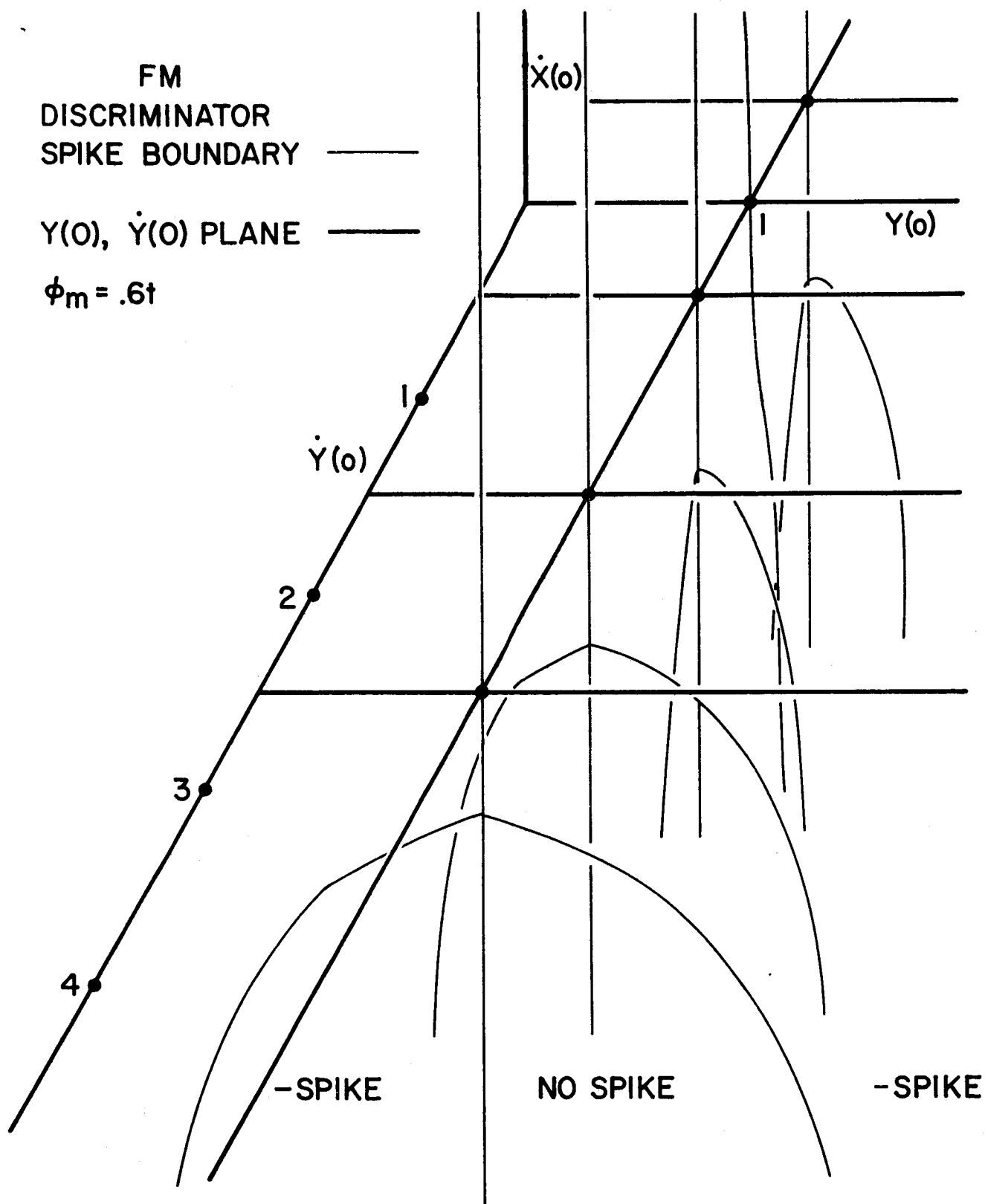


FIG 4

SPIKE BOUNDARY

SURFACES:

DISCRIMINATOR=

PLL (FIRST ORDER)

3db BANDWIDTH

5 RADIAN / SEC

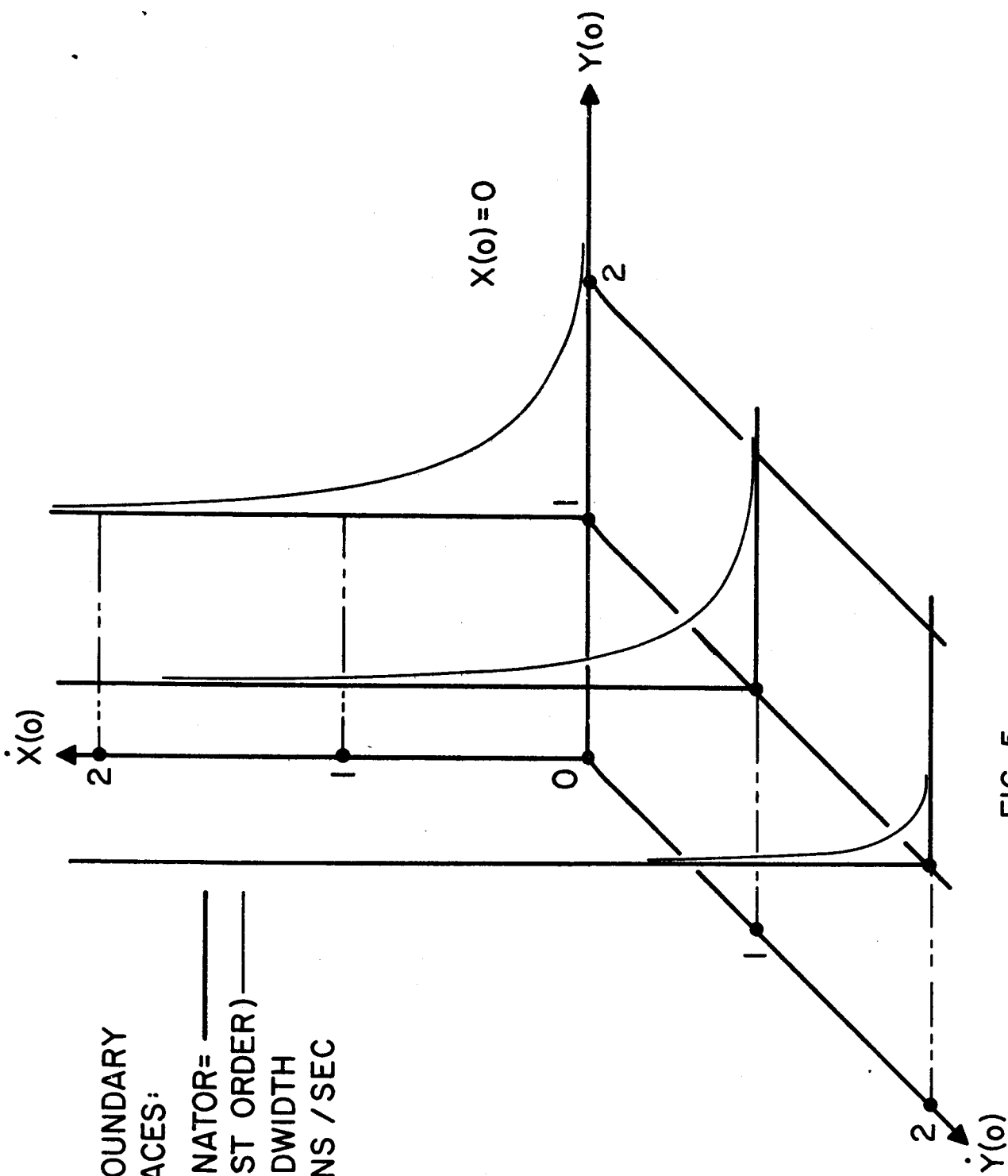


FIG. 5

SPIKE BOUNDARY
FOR PLL
(GAIN=5)

NOISES:
 $X(t)$ =QUADRATURE
 $Y(t)$ =IN PHASE

$$\phi_m = .6t$$

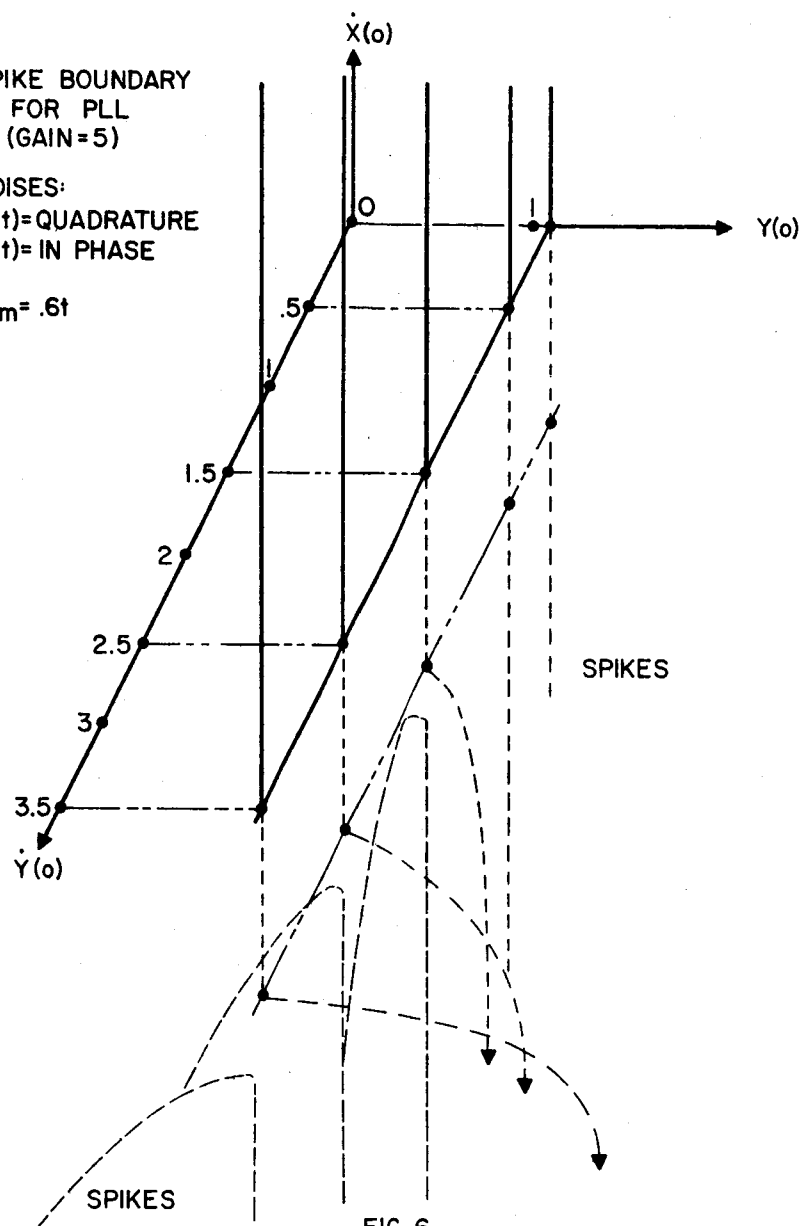


FIG. 6

SPIKE BOUNDARY
FOR SECOND ORDER
PLL WITH
MODULATION ———

$Y(0), \dot{Y}(0)$
PLANE ———

$$\phi_m = .6t$$

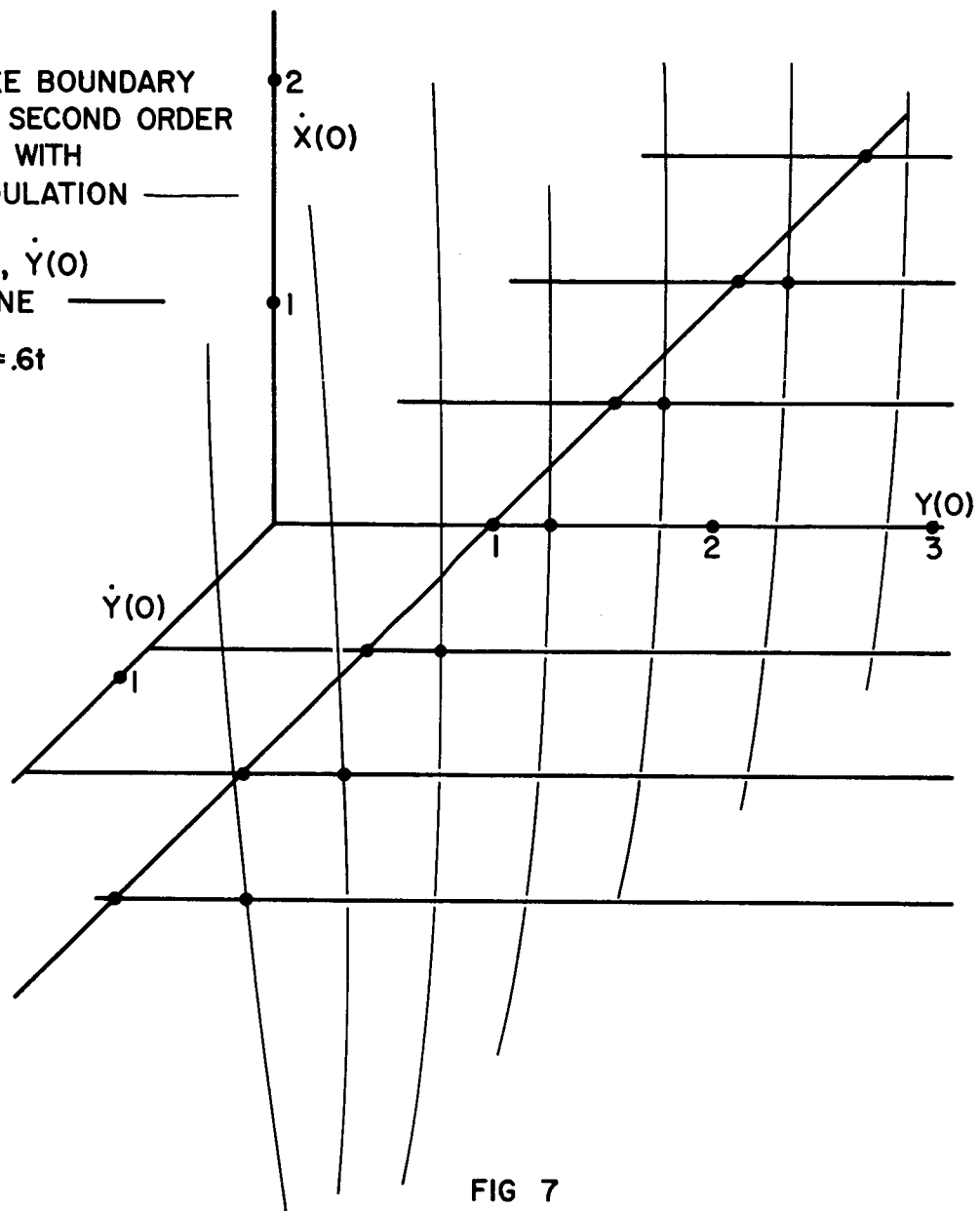


FIG 7

NORMALIZED EXPECTED NO. OF SPIKES PER SECOND

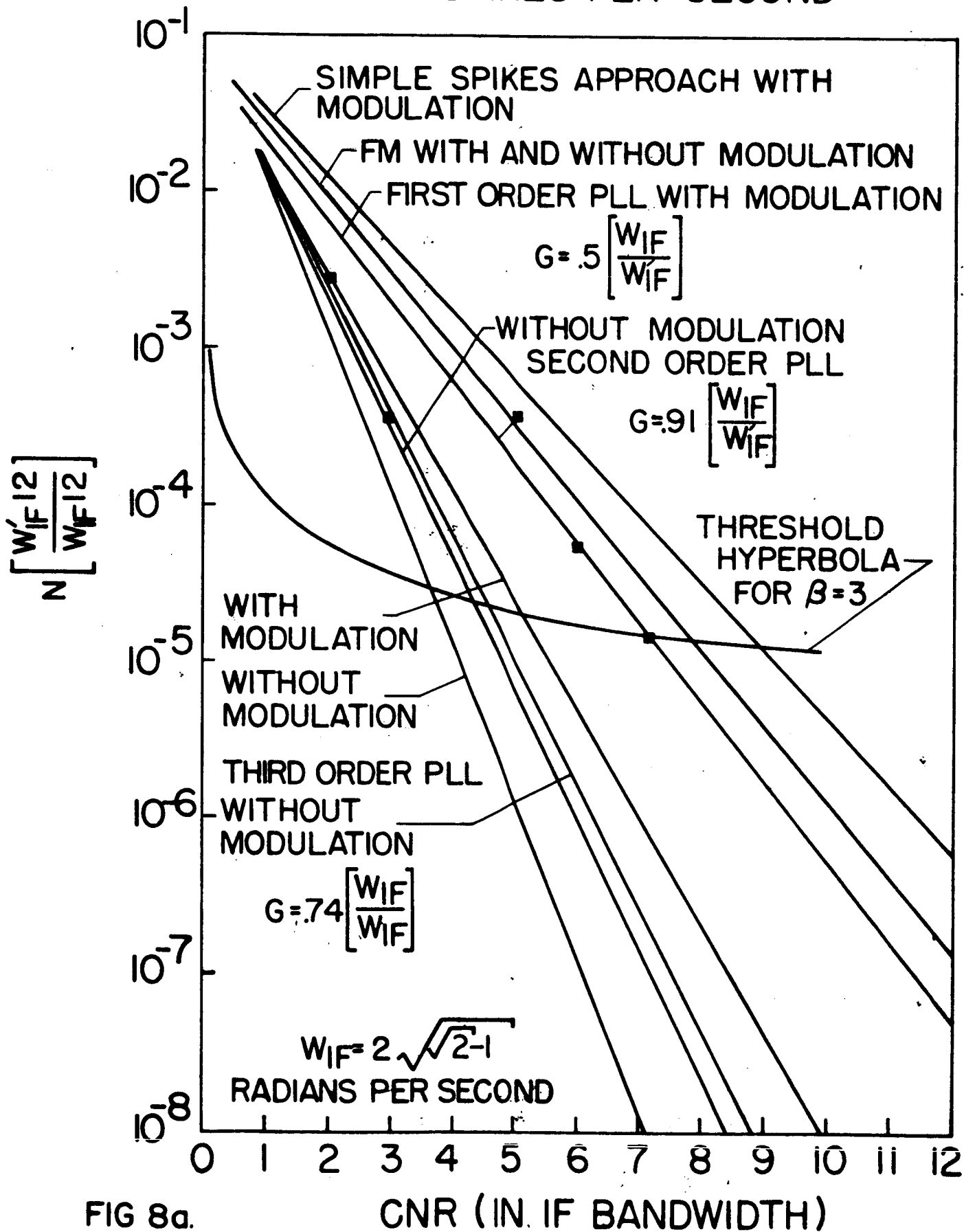


FIG 8a.

Fig. 8a.

NORMALIZED EXPECTED NO. OF SPIKES PER SECOND

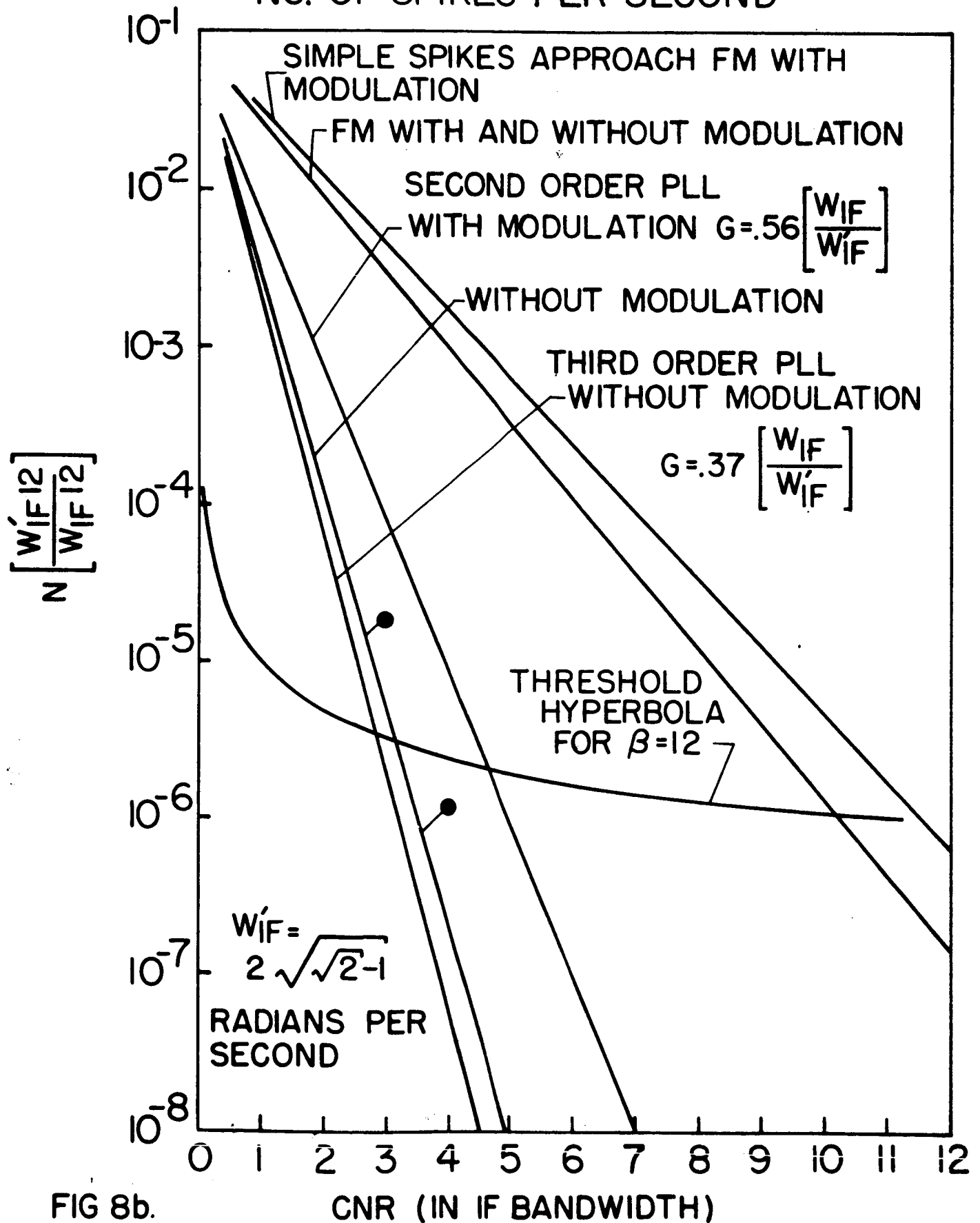


FIG 8b.

Fig 8b.

II. EQUIVALENCE OF FM THRESHOLD EXTENSION RECEIVERS

FM threshold extensions ^{are} achieved in FM detectors using the phase locked loop (PLL), the frequency locked loop (FLL), or the frequency demodulator with feedback. In this section the FLL and PLL are shown to ^{be} limiting forms of the FMFB.

1. Introduction

It is well known^{1, 2, 3, 4} that the FM noise threshold may be extended by employing an FM detector that uses a properly designed phase locked loop (PLL) or a frequency demodulator with feedback (FMFB). It has recently been demonstrated that the frequency locked loop⁵ (FLL) is also capable of threshold extension. In this section it shall be demonstrated that the defining equations for the PLL and FLL are limiting forms of the defining equations for the FMFB; hence rather than having three distinct devices capable of threshold extension, we have only one basic device (FMFB) from which the other two devices (PLL and FLL) are derivable. In particular it is shown that as the bandwidth of the internal IF filter of the FMFB is reduced to zero the FMFB and the PLL have the same defining equations. Conversely, as the bandwidth is increased without bound the equations for the FMFB and FLL are identical.

An interesting aspect of this equivalence is that a better physical understanding of the threshold extension mechanism of the FMFB may be obtained. Although some physical insight into the PLL and FLL has been gained, very little exists for the FMFB. In a previous paper⁶ it has been demonstrated that the PLL improves the FM noise threshold by not tracking (or "losing lock" during) many of the noise "clicks"⁷ that would normally appear at the output of a limiter-discriminator. In addition, it has been shown that the FLL improves the FM noise threshold by a "holding" mechanism that reduces the strength of many of the noise "clicks". Consequently, since an FMFB lies somewhere between the FLL and the PLL if its internal IF filter bandwidth is neither zero nor infinity the FMFB should achieve threshold extension by "losing lock" during some noise "clicks" reducing the strength of others.

This phenomenon was indeed observed by Cassara.⁹ He compared the outputs of an FMFB and a limiter-discriminator which were excited by the same unmodulated FM carrier plus narrow band noise (both centered about the same frequency ω_0) and noted that some of the noise "clicks" existing at the output of the limiter-discriminator did not exist at all at the output of the FMFB, while other noise "clicks" were reduced in strength or area. With an unmodulated carrier, no noise "click" appeared at the output of the FMFB which did not appear at the output of the limiter-discriminator.

Consequently demonstrating the equivalence of the defining equations of the three devices yields a starting point for the understanding of the FMFB. To begin the analysis the defining equations for the FLL and PLL are developed. The equation for the FMFB is then developed as a function of its internal IF filter, whose bandwidth is first increased without bound and then reduced to zero. Convergence of the FMFB equation to that of the FLL and PLL is thus demonstrated.

2. Frequency Locked Loop Equation

The block diagram of the baseband version of the FLL is shown in Figure 1. Here the input is assumed to be in the completely general form of a carrier centered at ω_0 modulated by an amplitude $a(t)$ and a phase $\psi(t)$. The amplitude term $a(t)$ arises when the FM carrier is added to narrow-band noise centered about ω_0 , whereas $\psi(t)$ consists of the desired FM modulation plus perturbations from the narrowband noise. Without loss of generality, the constants associated with the limiter-discriminator and amplitude demodulator are taken as unity, and the entire loop constant $B/2\alpha$ is associated with the loop filter whose impulse response is $h_0(t)$. The form of $B/2\alpha$ for the loop constant is chosen such that the equivalence between the FMFB and the FLL is more evident.

If the output of the loop is defined as $\hat{\phi}(t)$, then by proceeding around the loop one quickly obtains the defining equation for the FLL to be

$$\dot{\phi}(t) = \left\{ \left[\frac{a(t)B}{2\alpha} \right] \left[\dot{\psi}(t) - \dot{\phi}(t) \right] \right\} * h_o(t) \quad (2.1)$$

where * denotes convolution.

The block diagram of Figure 1 provides some insight into the threshold extending mechanism of the FLL. Clearly if $a(t)$ is small the closed loop bandwidth of the loop decreases and the output $\dot{\phi}(t)$ is permitted small variations (especially if the low pass loop filter has a pole close to the origin which it should have). However, as is known¹⁰, when a noise "click" occurs in $\dot{\psi}(t)$ which is a step of $\pm 2\pi$ in $\psi(t)$, $a(t)$ has a high probability of lying very close to zero; thus $\dot{\phi}(t)$ is "held" during the occurrence of a "click" which results in the "click" being suppressed at the output.

3. Phase Locked Loop Equation

The block diagram of the PLL is shown in Figure 2. Here the same input signal is assumed as for the FLL and the output signal is similarly defined as $\dot{\phi}(t)$. In addition without loss of generality the constant of the voltage controlled oscillator VCO is taken as unity and the entire loop constant B is associated with the output amplitude of the VCO. Here again one proceeds around the loop, recognizes that the loop filter rejects the second harmonic terms (in the vicinity of $2\omega_o$) appearing at the multiplier output, and writes the defining equation for the loop in the form

$$\dot{\phi}(t) = \left\{ \frac{a(t) B}{2} \sin [\psi(t) - \phi(t)] \right\} * h_o(t) \quad (2.2)$$

In this loop as in the FLL the closed loop bandwidth is controlled by $a(t)$.

Here however, during a "click" in $\dot{\psi}(t)$ and a step of $\pm 2\pi$ in $\psi(t)$, small values of $a(t)$ prevent $\dot{\phi}(t)$ or $\phi(t)$ from changing rapidly. Therefore as $\psi(t)$ varies by $\pm 2\pi \sin [\psi(t) - \phi(t)]$ passes through an entire cycle and returns to its starting point, thereby leaving the initial conditions of the PLL unchanged from those immediately preceding the "click". Thus the loop "loses lock" for a cycle and no "click" appears at the output. Only those steps in $\psi(t)$ during which $a(t)$ is reasonably large produce output "clicks" since the PLL is then able to track the steps in $\psi(t)$.

4. Frequency Demodulator with Feedback Equation

The block diagram of the FMFB is shown in Figure 3. Here again the input signal is identical with the one applied to the FLL and PLL and the output signal is again defined as $\dot{\phi}(t)$. Again the constants of the VCO and the discriminator are chosen as unity. The IF filter is assumed to be a single-pole filter (for stability) whose transfer function is given by

$$H_{IF}(s) = \frac{2s}{s^2 + 2\alpha s + \omega_2^2} = \mathcal{L}[h_{IF}(t)] \quad (2.3)$$

where ω_2 is the difference between the output frequency ω_1 of the "free running" VCO and the input frequency ω_0 , α is the distance of

the poles of $H_{IF}(s)$ from the imaginary axis in the complex s plane, and \mathcal{L} is the Laplace Transform operator.

The discriminator in the loop has no limiter and has the property that if its input $S_1(t)$ is given by

$$S_1(t) = \delta(t) \cos[\omega_2 t + \lambda(t)] \quad (2.4)$$

its output $S_2(t)$ is given by

$$S_2(t) = \delta(t) \dot{\lambda}(t) \quad (2.5)$$

A little thought readily shows that such a description is valid for any conventional discriminator not preceded by a limiter for which $\omega_2 - |\dot{\lambda}| \gg \delta(t)/\delta(t)$. In general the complete equation for $\dot{\varphi}(t)$ for the FMFB may be readily written down from the block diagram of Figure 3; however its form is so complex that little or no insight can be gained from it. Consequently in the following paragraphs only the two desired limiting forms of the FMFB are considered. First the bandwidth of $H_{IF}(s)$ is permitted to become large and then it is permitted to approach zero.

Large Bandwidth for Loop IF Filter. FMFB Approaches FLL.

As the bandwidth of the loop IF filter becomes large compared with the band of frequencies occupied by

$$\frac{a(t)B}{2} \cos [\omega_2 t + \psi(t) - \varphi(t)]$$

the filter output is an attenuated, but undistorted, version of its input which is given by

$$S_1(t) = \left(\frac{1}{\alpha} \right) \left(\frac{a(t)B}{2} \cos [\omega_2 t + \psi(t) - \phi(t)] \right) \quad (2.6)$$

where $(1/\alpha)$ is the transfer function of the IF filter in its pass-band.

Consequently the output of the discriminator is given by

$$S_2(t) = \frac{a(t)B}{2\alpha} [\dot{\psi}(t) - \dot{\phi}(t)] \quad (2.7)$$

from which the defining equation for the FMFB is readily obtained in the form

$$\dot{\phi}(t) = S_2(t) * h_o(t) = \left\{ \frac{a(t)B}{2\alpha} [\dot{\psi}(t) - \dot{\phi}(t)] \right\} * h_o(t) \quad (2.8)$$

Clearly Equations 2.1 and 2.8 are identical; hence the equivalence between the defining equations of the FMFB and FLL in this case is demonstrated.

It should be noted that Equation 2.8 is strictly valid only if the internal loop bandwidth increases without bound.[†] In practice however, since the input signal to the FMFB has already been band-limited by some external RF filter and since the multiplication of the input signal by the VCO output increases this band of frequencies by at most a factor of 2 or 3 in the vicinity of ω_2 , the bandwidth of the internal IF filter need be no more than twice as large as the bandwidth of the external RF filter to have the FMFB and the FLL perform in the same fashion.

[†] As the IF bandwidth is increased it is assumed that the out of band signals at the multiplier output, centered at $\omega_0 + \omega_1$, are still rejected.

Small Bandwidth for Loop IF Filter. FMFB Approaches PLL.

As the bandwidth of the loop IF filter becomes small compared with the band of frequencies occupied by

$$\frac{a(t)B}{2} \cos [\omega_2 t + \psi(t) - \varphi(t)]$$

the filter output is a strongly distorted version of its input. Some idea of the nature of this distortion is obtained by expanding the filter output in the form

$$\begin{aligned} S_1(t) &= \left\{ \left[\frac{a(t)B}{2} \right] [\cos[\psi(t) - \varphi(t)] \cos \omega_2 t \right. \\ &\quad \left. - \sin[\psi(t) - \varphi(t)] \sin \omega_2 t] \right\}^* h_{IF}(t) \\ &= \left[\left\{ \frac{a(t)B}{2} \cos[\psi(t) - \varphi(t)] \right\}^* h_L(t) \right] \cos \omega_2 t \\ &\quad - \left[\left\{ \frac{a(t)B}{2} \sin[\psi(t) - \varphi(t)] \right\}^* h_L(t) \right] \sin \omega_2 t \end{aligned} \quad (2.9)$$

where $h_L(t)$ is the impulse response of the low-pass equivalent filter of the narrow-band IF filter. In particular if $H_{IF}(s) = 2s/s^2 + 2\alpha s + \omega_2^2$ then

$$H_L(s) = \mathcal{L}[h_L(t)] = \frac{1}{s + \alpha} \quad (2.10)$$

Equation 2.9 may be rearranged still further to yield

$$S_1(t) = [C + c(t)] \cos \omega_2 t - [D + d(t)] \sin \omega_2 t \quad (2.11)$$

where C and D are the average or dc values of the respective coefficients of the $\cos \omega_2 t$ and $\sin \omega_2 t$ terms in Equation 2.9, and $c(t)$ and $d(t)$ are the respective values of the coefficients less their average values. If the RF filter preceding the loop is symmetric about ω_0 and if $\overline{\varphi(t)} = 0$, it is apparent from symmetry considerations that $\overline{\psi(t)} = 0$ and $\overline{a(t) \sin[\psi(t) - \varphi(t)]} = 0$; hence

$D = 0$. On the other hand, C is clearly not equal to zero; consequently Equation (2.11) may be further rearranged to yield

$$S_1(t) = \sqrt{[C + c(t)]^2 + [d(t)]^2} \cos \left[\omega_2 t + \tan^{-1} \frac{d(t)}{C + c(t)} \right] \quad (2.12)$$

from which follows

$$S_2(t) = \frac{[C + c(t)] \dot{d}(t) - d(t) \dot{c}(t)}{\sqrt{[C + c(t)]^2 + [d(t)]^2}} \quad (2.13)$$

It is apparent at this point that as the bandwidth of the IF filter (2α) approaches zero $c(t)$ and $d(t)$ become vanishingly small compared with C (more and more of the ac component is filtered while the dc component remains unchanged) and Equation (2.13) reduces to the limiting form

$$S_2(t) = \dot{d}(t) = \frac{d}{dt} \left[\left\{ \frac{a(t)B}{2} \sin[\psi(t) - \varphi(t)] \right\} * h_L(t) \right] \quad (2.14)$$

In addition, as $\alpha \rightarrow 0$, $H_L(s) \rightarrow 1/s$ which is a pure integrator; hence convolution with $h_L(t)$ in Equation 2.14 corresponds to integration which cancels with the differentiation operation to yield

$$S_2(t) = \frac{a(t)B}{2} \sin[\psi(t) - \varphi(t)] \quad (2.15)$$

and finally

$$\dot{\varphi}(t) = S_2(t) * h_o(t) = \left\{ \frac{a(t)B}{2} \sin[\psi(t) - \varphi(t)] \right\} * h_o(t) \quad (2.16)$$

Clearly Equations 2.16 and 2.2 are identical; hence the equivalence between the defining equations of the FMFB and the PLL in this case is demonstrated.

Although the loop IF bandwidth must theoretically reach zero to have the FMFB function as a PLL, it has been found experimentally⁹ that for IF bandwidths less than 1/10 of the external RF filter bandwidth the FMFB functions, with respect to a noise-corrupted input carrier, in essentially the same fashion as the PLL.

Several interesting observations may be made at this point. First, the FMFB may have an arbitrarily narrow loop IF filter bandwidth and still successfully demodulate an input FM signal. This is quite obvious since the PLL is capable of performing such a demodulation. Previously it was believed by many writers^{1, 3} that the loop IF filter must have a bandwidth at least equal to twice the frequency range occupied by the modulation information.

Secondly, with a sufficiently narrow loop IF filter bandwidth the FMFB has all of the "loss of lock" problems possessed by the PLL. Consequently large deviations of the input carrier in the presence of noise are capable of throwing the FMFB "out of lock" with the result of a large number of signal induced "clicks". On the other hand, for wide loop IF bandwidths the FMFB can never "lose lock". This is obvious since the PLL (which the FMFB

approaches, cf. Figure 1) has no VCO and therefore no mechanism by which to lose lock. Perhaps some intermediate value of loop IF bandwidth combines the best features of the PLL and FLL.

5. Conclusion

In this section it has been demonstrated that the defining equations of the FMFB degenerate into the equations for the FLL and PLL as the loop IF filter bandwidth of the FMFB approaches infinity or zero respectively. Consequently a possibility of further physical understanding of the FMFB may be obtained by approaching its operation from the limits of FLL operation on one end and PLL operation on the other. More significant, however, is the realization that the three basic threshold extension receivers are equivalent with respect to their defining equations to the single device, the FMFB.

References

1. L.H. Enloe, "Decreasing the Threshold in FM by Frequency Feedback", Proc. IRE, Vol. 50, Jan. 1962.
2. D.L. Schilling and J. Billig, "A Comparison of the Threshold Performance of the Frequency Demodulator Using Feedback and the Phase Locked Loop", Rec. 1965 International Space Electronics Symp., p. 3-E1.
3. M. Schwartz, W.R. Bennett, and S. Stein, "Communication Systems and Techniques", Chapter 3, McGraw-Hill, 1966.
4. P. Frutiger, "Noise in FM Receivers with Negative Frequency Feedback", Proc. IEEE, Vol. 54. November 1966
5. K.K. Clarke and D. T. Hess, "Frequency Locked Loop FM Demodulator" IEEE Trans. on Comm. Tech., Vol. Com-15, August 1967, pp.518-524.
6. D. T. Hess, "Cycle Slipping in First Order Phase Locked Loops". IEEE Trans. on Comm. Tech., April 1968.
7. S.O. Rice, "Noise in FM Receivers", Time Series Analysis, M. Rosenblatt, Ed. New York: Wiley, 1963, Chapter 25.
8. K.K. Clarke and D. T. Hess, Ibid.
9. F. Cassara, "FM Demodulator with Feedback", MS Project Report, Polytechnic Institute of Brooklyn, June 1968.
10. L. Calandrino and G. Immovilli, "Coincidence of Pulses in Amplitude and Frequency Deviations", Alta Frequenza, English Issue No. 3, Vol. 36, August 1967.

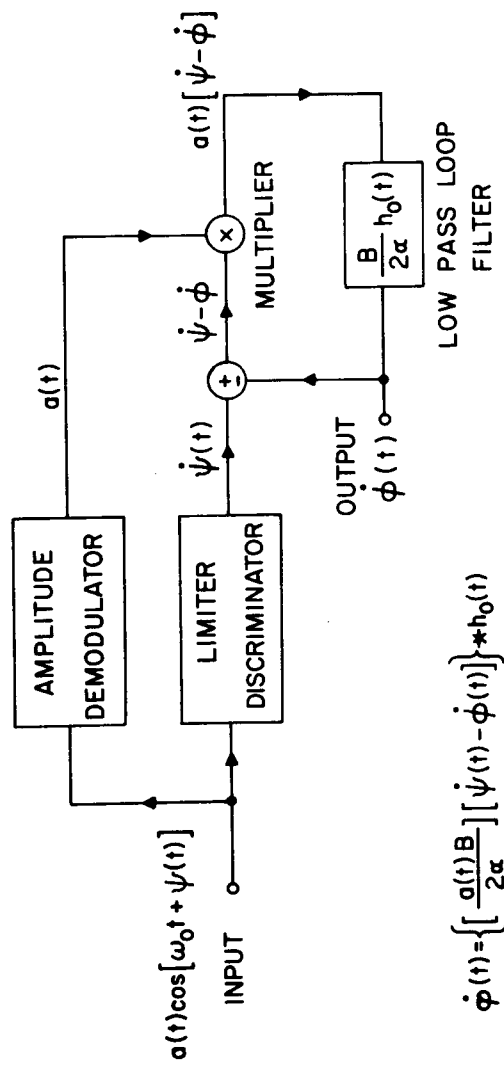
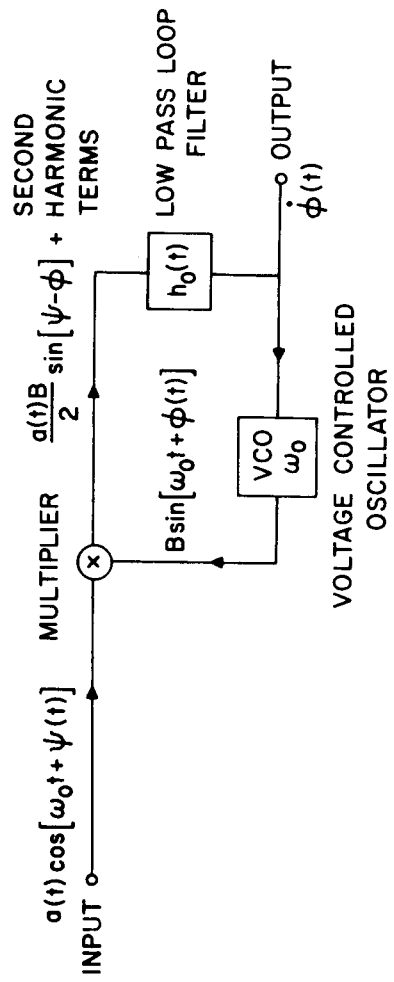


FIGURE 1 BLOCK DIAGRAM OF FREQUENCY LOCKED LOOP



$$\dot{\phi}(t) = \left\{ \frac{a(t)B}{2} \sin[\psi(t) - \phi(t)] \right\} * h_0(t)$$

FIGURE 2 BLOCK DIAGRAM OF PHASE LOCKED LOOP.

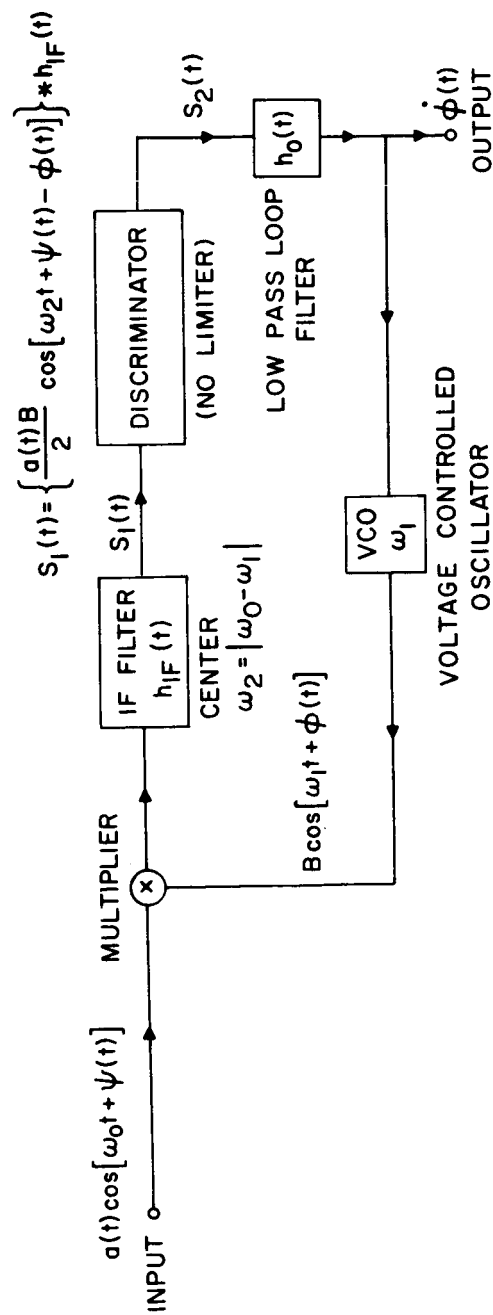


FIGURE 3 BLOCK DIAGRAM OF FREQUENCY DEMODULATOR WITH FEEDBACK

III.

FM MULTIPATH INTERFERENCE1. Introduction

We are concerned with the effects produced when a sinusoidally-modulated FM signal

$$e_1(t) = \cos[w_c t + \beta \sin pt] \quad (3.1)$$

is received in addition to a delayed, attenuated echo of the signal

$$e_2(t) = \rho \cos[w_c(t-\Delta t) + \beta \sin p(t-\Delta t) + \phi] \quad (3.2)$$

Here, ρ is the relative echo strength (assumed less than one), Δt is the echo delay time, w_c and p are the carrier and modulation radian frequencies respectively, β is the modulation index, and ϕ is an arbitrary phase added by the mechanism of the echo path. The total received signal is

$$e(t) = e_1(t) + e_2(t) \quad (3.3)$$

The echo creates a characteristic interference in the output of the discriminator. The discriminator consists of an ideal differentiator and an ideal envelope detector. The effect of a low-pass filter will be discussed in Section 4.

The discriminator yields output¹ (for $\rho < 1$, the case when the echo is weaker than the principal received signal)

$$\Delta w \cos pt + 2 \Delta w \sin \frac{p\Delta t}{2} \sin p(t - \frac{\Delta t}{2}) \rho \frac{\rho + \cos \psi}{1 + 2\rho \cos \psi + \rho^2}, \quad (3.4)$$

where ψ is the instantaneous phase difference between the principal and delayed signals,

$$\psi = \phi - w_c \Delta t - 2\beta \sin \frac{p\Delta t}{2} \cos p(t - \frac{\Delta t}{2}) \quad (3.5)$$

and Δw is the maximum instantaneous radian frequency deviation,

$$\Delta w = p\beta.$$

The signal $\Delta w \cos pt$ is the (desired) information received when no echo is present, and the remainder is the interference,

$$w_i(t) = 2\Delta \sin \frac{p\Delta t}{2} \sin p(t - \frac{\Delta t}{2}) \rho \frac{\rho + \cos \psi}{1 + 2\rho \cos \psi + \rho^2}. \quad (3.6)$$

2. Characteristics of the Interference.

The demodulated signal plus multipath interference, 3.4, consists of the expected sinusoid plus pulses of variable height. A typical wave form of the interference alone is illustrated in Fig. 2.1. A pulse occurs each time the function (3.5) passes through an odd multiple of π ; at this

1. See, for example, Philip P. Panter, Modulation, Noise, and Spectral Analysis Applied to Information Transmission; New York, McGraw-Hill, 1965, pp. 364 ff.

point the function

$$f(\psi) = \rho \frac{\rho + \cos \psi}{1 + 2 \rho \cos \psi + \rho^2} \quad (3.7)$$

reaches a (negative) peak.

An estimate of the number of these pulses in each cycle of the modulation is just twice the peak-to-peak swing of $\psi(t)$ divided by the interval between peaks of $f(\psi)$, or 2π . (The factor of 2 occurs because $\psi(t)$ passes through its range twice in each modulation cycle.) Thus, number of pulses/modulation cycle = $N = \frac{4}{\pi} \beta \left| \sin p \frac{\Delta t}{2} \right|$. (3.8)

It must be emphasized that this is not a precise result. The actual number of pulses in a modulation cycle is dependent upon the time-independent term in $\psi(t)$,

$$\theta \equiv \phi - w_c t. \quad (3.9)$$

In any case, the exact value of N differs by less than one from that given by 3.8. In addition, if it is assumed that θ is a random variable of uniform density over some interval of 2π , the expected number of pulses per modulation cycle is given exactly by 3.8.

The maximum value of N occurs when the echo modulation is 180° out of phase with the modulation of the primary signal. In this case, $\left| \sin p \frac{\Delta t}{2} \right| = 1$ and $N = \frac{4}{\pi} \beta$.

As ρ becomes larger, the amplitude of the pulses increases; as $\rho \rightarrow 1$, the interference becomes impulsive. This is easily deduced from the following facts:

$$\int_0^{2\pi} \rho \frac{\rho + \cos \psi}{1 + \rho^2 + 2\rho \cos \psi} d\psi = 0, 0 \leq \rho < 1 \quad (3.10)$$

and

$$\lim_{\rho \rightarrow 1} \rho \frac{\rho + \cos \psi}{1 + \rho^2 + 2\rho \cos \psi} = \frac{1}{2}, \quad \psi \neq n\pi, n \text{ odd}. \quad (3.11)$$

$$\text{So, for } \rho = 1, f(\psi) = \frac{1}{2} - \pi \sum_{n \text{ odd}} \delta(\psi - n\pi)$$

Similarly, the interference $w_i(t)$ (3.6) becomes

$$2\Delta w \sin \frac{p\Delta t}{2} \sin p(t - \frac{\Delta t}{2}) \left[\frac{1}{2} - \pi \sum_{n \text{ odd}} \delta(\psi(t) - n\pi) \right] \quad (3.12)$$

Here, the impulses are not evenly spaced in time; still, the number of impulses in a modulation cycle is approximately

$$N = \frac{4}{\pi} \beta \left| \sin p \frac{\Delta t}{2} \right|. \quad (3.13)$$

Since $\delta(\psi(t)) = \sum_i \frac{\delta(t - t_i)}{|\psi'(t_i)|}$, where the t_i satisfy $\psi(t_i) = 0$,

and $\psi'(t) = 2\Delta w \sin \frac{p\Delta t}{2} \sin p(t - \frac{\Delta t}{2})$, . . becomes

$$2\Delta w \sin p \frac{\Delta t}{2} \sin p(t - \frac{\Delta t}{2}) + \pi \sum_i (\pm \delta(t_i)) \quad (3.14)$$

where now the t_i are the times that $\psi(t)$ passes through an odd multiple of π . The impulses are positive when the sign of $[\sin p \frac{\Delta t}{2} \sin p(t_i - \frac{\Delta t}{2})]$ is negative; the impulses are negative otherwise. (The number of positive and negative pulses is equal.)

Note that the impulses in 3.14 have area $\pm\pi$. This is in contrast with the impulses produced by additive noise, which have area $\pm 2\pi$. This is explained by the phasor diagrams in Fig. 2.2, which contrasts the two types of interference.

While the direction of noise pulses is generally in opposition to the modulation signal, no such generalization can be made for multipath interference. If we again assume that the constant phase difference between primary signal and echo is uniformly random over some interval of width 2π , the probability of a multipath pulse in a short interval dt is

$$H(t) = \frac{|\psi'(t)|}{2\pi} dt ,$$

or

$$H(t) = \frac{1}{\pi} \left| \Delta w \sin p \frac{\Delta t}{2} \sin p(t - \frac{\Delta t}{2}) \right| dt \quad (3.15)$$

Positive pulses occur only when the sign of $\sin p \frac{\Delta t}{2} \sin p(t - \frac{\Delta t}{2})$ is negative; otherwise, the pulses are negative. Fig. 2.3 illustrates the regions of positive and negative pulses as the delay time, Δt , varies.

Time regions of positive and negative pulses as Δt varies. The integral of (3.15) over a modulation cycle is just the total number of pulses per cycle given by (3.8).

3. Interference Power

To characterize the intensity of the interference (3.6), it is helpful to know the power of the interference. Here, the "power" of a time function $g(t)$ of period T is defined as

$$\frac{1}{T} \int_0^T [g(t)]^2 dt$$

while the "energy" of a (nonperiodic) function $h(t)$ is defined as

$$\int_{-\infty}^{\infty} |h(t)|^2 dt$$

The exact value of the interference power is not simple to find, but if we (once again) average over the quantity $\theta \neq \phi - w_c \Delta t$, we get

$$\frac{1}{2\pi} \int_0^{2\pi} \frac{1}{T} \int_0^T [w_i(t)]^2 dt = (\Delta w \sin p \frac{\Delta t}{2})^2 \frac{\rho^2}{1-\rho^2} \quad (3.16)$$

Note that this power becomes infinite as $\rho \rightarrow 1$. This is to be expected, since impulses have infinite power. In a real system, of course, the pulses (and power) would be limited by the discriminator output filter and perhaps by amplitude failure of the discriminator as well. The effect of low-pass filtering of the interference is considered in the next section.

4. Effect of Filtering on Interference

As echo strength increases, interference pulses become narrower, with a corresponding increase in bandwidth. At some point, the effect of output filtering on the interference power will become significant.

To determine the effect on interference power of output filtering, the following assumption and approximations are made :

- (1) The filter is an ideal low-pass filter with cutoff frequency f_0 , i. e.

$$H(f) = 1, \quad |f| < f_0; \quad H(f) = 0 \quad \text{elsewhere}.$$

- (2) The filter bandwidth is sufficiently wide so that the energy of all pulses may be added independently.

- (3) The pulses are produced by the function $A(t) f(\psi(t))$, where

$$A(t) = 2\Delta \sin p \frac{\Delta t}{2} \sin p(t - \frac{\Delta t}{2})$$

and $f(\psi)$ and $\psi(t)$ are given by (3.7) and (3.5), respectively.

It is assumed that, if a pulse occurs with peak at $t = t_i$, it may be considered to have the following form :

$$A(t_i) f(|\psi'(t_i)| (t - t_i) - \pi), \quad |\psi'(t_i)| |(t - t_i)| < \pi \quad (3.7)$$

Thus, the time-and amplitude-scales of the pulses are held constant throughout the pulse.

- (4) The familiar assumption about the randomness of the constant phase difference, θ , will be made.

Of these assumptions, (2) is probably the most restrictive. Pulses can theoretically occur arbitrarily close in time if the total signal phasor reverses direction in the vicinity of the origin, Fig. 4.1.

These double-pulses are of opposite polarity and tend to have relatively small amplitude, and therefore should constitute only a small portion of interference power. Barring this phasor reversal case, the minimum time between pulses of like polarity is $\frac{1}{2\pi} |\psi'(t)|_{\max}$, or $\frac{1}{2\Delta f}$, where Δf is the maximum frequency deviation. Here we are requiring that the audio bandpass be on the order of the RF bandpass.

The other assumptions are not very restrictive. One might suspect that assumption (3), concerning the pulse shape, would be the source of considerable error. It will be seen, however, that the averaged (over θ) power calculated with this assumption yields the (known) correct result for the case in which the output filter is omitted.

To find the power of the filtered interference, we need just find the filtered energy of an isolated pulse, and sum over a modulation cycle, taking into account the expected density of pulses (3.15).

To calculate the filtered energy of a single pulse, we use the Fourier series expansion² of $f(a\psi)$:

$$f(a\psi) = \rho \frac{\rho + \cos a\psi}{1 + \rho^2 + 2\rho \cos a\psi} = \rho \cos a\psi - \rho^2 \cos^2 a\psi + \rho^3 \cos^3 a\psi \dots \quad (3.18)$$

Each term has power $\frac{\rho^2}{2}$, $\frac{\rho^4}{2}$, $\frac{\rho^6}{2}$,

² Ibid, p. 252.

If the filter passes the harmonics up to (radian) frequency na , then

$$\text{power} = \frac{1}{2} \sum_{j=1}^n \rho^{2j} = \frac{1}{2} \frac{\rho^2}{1-\rho^2} [1-\rho^{2n}] \quad (3.19)$$

or the energy in a single, filtered pulse is just (power) . (period) or

$$\frac{1}{2} \frac{2\pi}{a} \frac{\rho^2}{1-\rho^2} [1-\rho^{\frac{4\pi f_0}{a}}] 2\pi f_0 = na \quad (3.20)$$

In the multipath interference case, a is a time function, namely,

$$a = |\psi'(t)| = |2\Delta w \sin p \frac{\Delta t}{2} \sin \rho(t - \frac{\Delta t}{2})| \quad (3.21)$$

and in addition the pulse is multiplied by an amplitude function $A(t)$,

which is also equal to $\psi'(t)$.

The actual energy of the pulse is, therefore,

$$\begin{aligned} (\psi'(t))^2 & \frac{\pi}{|\psi'(t)|} \frac{\rho^2}{1-\rho^2} \left[1-\rho^{\frac{4\pi f_0}{|\psi'(t)|}} \right] \\ &= \pi |\psi'(t)| \frac{\rho^2}{1-\rho^2} \left[1-\rho^{\frac{4\pi f_0}{|\psi'(t)|}} \right] \end{aligned} \quad (3.22)$$

The probability of a pulse in an interval $(t, t+dt)$ was shown to be

$$\frac{1}{\pi} |\psi'(t)| dt, \quad (3.15)$$

if the two-path phase difference, θ , is uniformly random over some 2π interval; the energy of an isolated pulse is given by 3.22 so the power, averaged over θ , is

$$\frac{p}{2\pi} \int_0^{2\pi} 2 \left[\Delta w \sin p \frac{\Delta t}{2} \sin p \left(t - \frac{\Delta t}{2} \right) \right]^2 \frac{\rho^2}{1-\rho^2} \left[1 - \frac{f_o}{\Delta f \rho \left| \sin p \frac{\Delta t}{2} \right| \sin p \left| t - \frac{\Delta t}{2} \right|} \right] dx$$

$$= \left[\Delta w \sin p \frac{\Delta t}{2} \right]^2 C \quad (3.23)$$

where

$$C = 1 - \frac{4}{\pi} \int_0^{\frac{\pi}{2}} \sin^2 x \exp \left[- \frac{f_o \log e 1/\rho}{\Delta f \left| \sin p \frac{\Delta t}{2} \right| \sin x} \right] dx \quad (3.24)$$

is the attenuation of the interference by the filter.

The integral in (3.24) is well behaved for $0 \leq \rho \leq 1$. For $f_o \rightarrow \infty$ or $\rho \rightarrow 1$, $C = 1$, which gives the expected result (3.16) for no output filter.

For $0.0 < \frac{f_o \log e 1/\rho}{\Delta f \left| \sin p \frac{\Delta t}{2} \right|} < 1$, C is given by

$$C = \frac{4}{\pi} \frac{f_o}{\Delta f} \frac{\log e 1/\rho}{\Delta f \left| \sin p \frac{\Delta t}{2} \right|} \quad (3.25)$$

This approximation applies when great attenuation of the interference by the filter is experienced.

A plot of C against $y = \frac{f_o}{\Delta f} \frac{\log e 1/\rho}{\left| \sin p \frac{\Delta t}{2} \right|}$ is shown in Fig. 4.2.

It is now possible to calculate the power of the filtered multipath interference. Since the information output signal is $\Delta w \cos pt$, with power $(\Delta w)^2/2$, the noise-to-signal power ratio is

$$2 \left(\sin p \frac{\Delta t}{2} \right)^2 \frac{\rho^2}{1-\rho^2} C \quad (3.26)$$

In Fig. 4.3 equation (3.26) has been plotted for the special "worst case" when the echo modulation is 180° out of phase with that of the primary path signal. In this case, $\sin p \frac{\Delta t}{2} = 1$. Various values of filter bandwidth f_0 , normalized with respect to the maximum carrier frequency deviation Δp , are shown.

It is seen that attenuation is appreciable for all values of ρ . This emphasizes the wideband character of the interference, even when the interference pulses are far from being impulses. For values of $|\sin p \frac{\Delta t}{2}| < 1$, the interference power is decreased by the square of this quantity, but the effective filter bandwidth is multiplied by the reciprocal of this quantity.

Recursive Techniques

Introduction

Recursive techniques provide a rather simple way of handling both analytically and for the purpose of implementation the detection, estimation, demodulation, smoothing and data reduction of various types of signals. They permit the consideration of more realistic system models, and lead directly to computer algorithms for processing the data in the desired way.

A recursive method can be described as a scheme whereby the processing of the signals (i) takes place in real time and (ii) uses previously calculated results for extended processing rather than all the data. For the most part the analytical results are either in the form of a finite difference or a differential equation. The former being used for digital computer processing, the latter having its application in analog processing.

The early organized work in recursive processing is due to Kalman⁽¹⁾ (1960) and was mostly concerned with linear, minimum mean square estimation or filtering of signals in white noise. While this problem is significant in its own right there remain many more difficult problems of an immediate practical interest. These include :

- (1) Detection and estimation of arbitrary signal in noise. Non white, non-Gaussian noise, time varying channels, optimum and sub-optimum but real time realizeable demodulation and other nonlinear processing.
- (2) Adaptive techniques and the application of recursive methods to simplify and modify the processing operations as measured conditions on the channel change. This would be very impractical and cumbersome without recursive methods.

It is important to note that while Kalman's approach requires very little of the statistics of the signals and noises that are operated upon,

(only second moments) this is not true for the problems cited here. The recursive method, generally applied, uses more of the statistical structure of the signals and noise, but since the end result requires only present data and only previous estimates, offers significant advantages in simplicity, and in minimizing memory requirements.

Detection of Signals in Noise

As an example of a recursive method which has been recently worked out⁽²⁾ we will compare the conventional approach to the problem of detecting binary signals in correlated noise to the recursive approach. It is not to be inferred that this example is unique nor that the recursive method applies only to this problem.

Problem: Detection of Signals in additive, non-white noise with minimum probability of error.

Observations: $Y(J) = S_i(J) + X(J) \quad 0 \leq J \leq t$
 $i = 1, 2$

Given: $S_i(t) \quad i = 1, 2$ and "statistic" of $X(t)$

Constraints on Signal Processing: only discrete samples (or its derivatives) are available e. g. $Y(\Delta), Y(2\Delta), \dots Y(n\Delta)$ or

e. g. $Y(\Delta), Y^1(\Delta), Y(2\Delta), Y^1(2\Delta), \dots Y(n\Delta), Y^1(n\Delta)$

etc.

Optimum solution: (Likelihood Ratio)

$$L(Y(t)) = \frac{f_Y(y(J), J \leq t/S_1)}{f_Y(y(J), J \leq t/S_2)} > b_o$$

If $L(Y(t))$ exceeds the threshold b_o , decide S_1 otherwise decide S_2

Conventional approach using discrete samples when $N(t)$ is Gaussian with known covariance function

$$\underline{Y} = \begin{bmatrix} Y(\Delta) \\ Y(2\Delta) \\ \vdots \\ Y(n\Delta) \end{bmatrix}; C_{(n)} = E \underline{X} \underline{X}^T$$

The test statistic ($\log L(\underline{Y})$) is

$$\theta_n = \underline{Y}^T C_{(n)}^{-1} (\underline{S}_1 - \underline{S}_2)$$

The signal to noise ratio is

$$\lambda_n = (\underline{S}_1 - \underline{S}_2)^T C_{(n)}^{-1} (\underline{S}_1 - \underline{S}_2)$$

The minimum error probability is

$$\min P_n(E) = \frac{1}{2} \operatorname{erfc} \frac{1}{2} \sqrt{\lambda_n}$$

Problems with conventional approach

- 1) The matrix C_n that must be inverted is usually very large ($n = 10^3$).
- 2) All the observations \underline{Y} must be stored.
- 3) Taking an additional observation increases the dimension of the problem by 1 requiring

- a) A new matrix inversion $C_{(n+1)}^{-1}$
 - b) A new computation of the test statistic θ_n
 - c) A new computation of the $\min_{n+1} P(E)$
- 4) The memory requirements and computational work grows very rapidly with the number of samples taken.
- 5) The formulation does not lend itself to sequential or null-zone techniques.
- 6) The test statistics (likelihood ratio) can be conveniently written for Gaussian noise only.
- 7) In the continuous processing of the received signals, the optimum processor must be found by solving an integral equation. Explicit solutions are generally not available nor is the minimum $P(E)$.

Recursive Approach

Assume the noise is generated by

$$L \{X(t)\} = \left(\frac{d^k}{dt^k} + a_{k-1}(t) \frac{d^{k-1}}{dt^{k-1}} + \dots + a_1(t) \frac{d}{dt} + a_0 \right) X(t) = W(t)$$

$W(t)$ is a white process with covariance function $\eta_0 \delta(t_1 - t_2)$

[Rational Spectral Density noise is a special case]

$$\underline{\dot{X}}(t) = A(t) \underline{X}(t) + \underline{b}W(t)$$

e with state vectors

$$\underline{X} = \begin{bmatrix} X(t) \\ \vdots \\ X(t) \\ \vdots \\ \vdots \\ X^{(k-1)}(t) \end{bmatrix}, \quad A = \begin{bmatrix} 0 & 1 & 0 & \dots & 0 \\ 0 & 0 & 1 & \dots & 0 \\ \dots & \dots & \dots & \dots & \dots \\ -a_0(t) & -a_1(t) & \dots & -a_{k-1}(t) \end{bmatrix}, \quad \underline{b} = \begin{bmatrix} 0 \\ 0 \\ \vdots \\ \vdots \\ 1 \end{bmatrix}$$

$\underline{X}(t)$ is vector-Markov.

The test statistic then satisfies the difference equation:

$$\theta_n = \theta_{n-1} + 2(\underline{S}_n - B\underline{S}_{n-1})^T K^{-1} (\underline{Y}_n - B\underline{Y}_{n-1})$$

$$\theta_0 = 2\underline{S}_0^T C_0^{-1} \underline{Y}_0$$

where

$$B = C_\Delta C_0^{-1} ; \quad C_\Delta = E Y(t+\Delta) X^T(t)$$

$$K = C_0 - C_\Delta C_0^{-1} C_\Delta^T$$

The mechanization is shown in Figure 1.

Note: 1) Order of matrices is $k \ll n$.

2) B and K do not depend on n (They are constants in the recursive process).

Furthermore,

$$\lambda_n = \underline{S}_0^T C_0^{-1} \underline{S}_0 + \sum_{k=1}^n (\underline{S}_k - B_k \underline{S}_{k-1})^T K_k^{-1} (\underline{S}_k - B_k \underline{S}_{k-1}) .$$

Advantages of Recursive Approach

- 1) The only matrix that must be inverted is K and is usually small (3 or 4) .
- 2) Once K is inverted, it is the same no matter how many samples are taken.
- 3) Only the previous observation of \underline{Y} must be stored thereby considerably reducing memory requirements. The memory requirement does not grow with the data taken.
- 4) The difference equation lends itself to sequential or null-zone or feedback communications since the test statistic may be updated with only the addition of new data. Also, the closed-form expressions for the signal to noise ratio (and $P(E)$) may be used to optimize the performance of any such schemes.
- 5) The test statistic has a similar form even for non-gaussian noise statistics.
- 6) In the continuous case (not discussed here) the mechanization always yields realizable optimum solutions which may be implemented in a straight-forward, practical way.

Extensions and Further Promising Research Areas

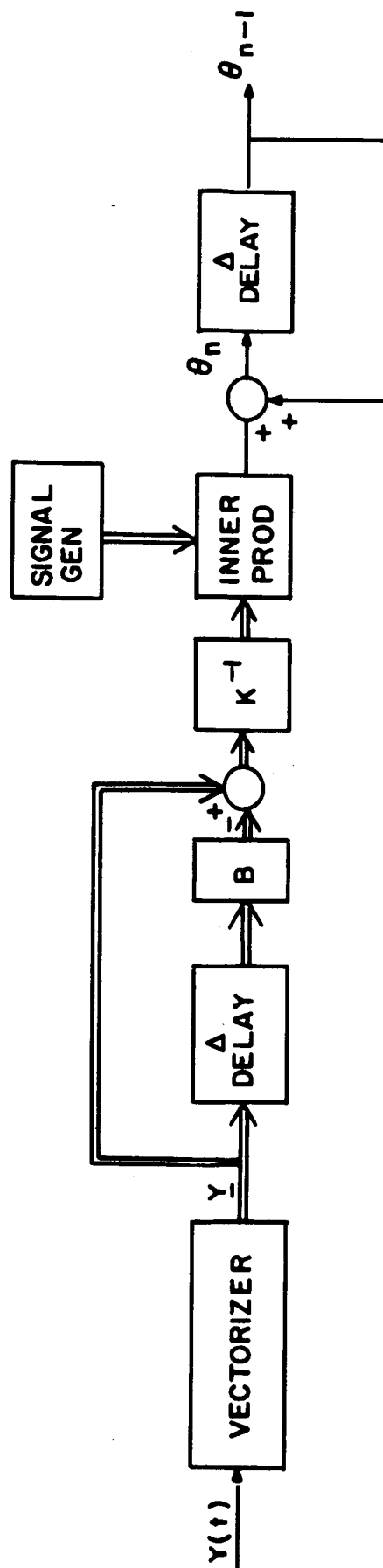
The above example is but one special, albeit important application of recursive techniques. The results already obtained can be immediately applied to a much larger class of problems that simplify the detection of signals in Gaussian noise. For example, the problems involved in pattern recognition, detection of stochastic signals, nonstationary systems and m -ary detection can all be treated in the same framework. Some unexplored areas of great practical and theoretical interest where the state-

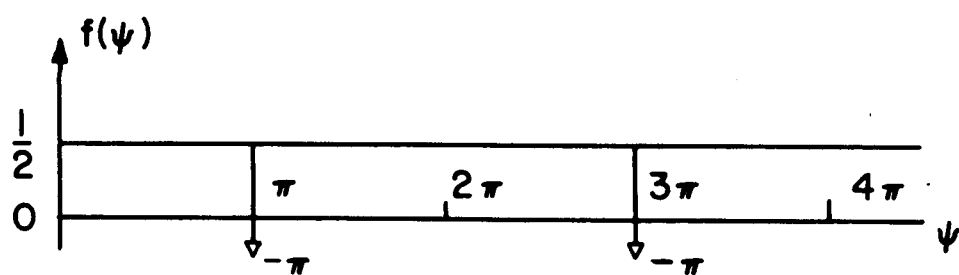
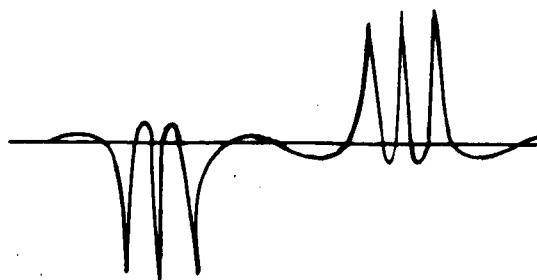
variable approach for recursive formulation are expected to yield results are :

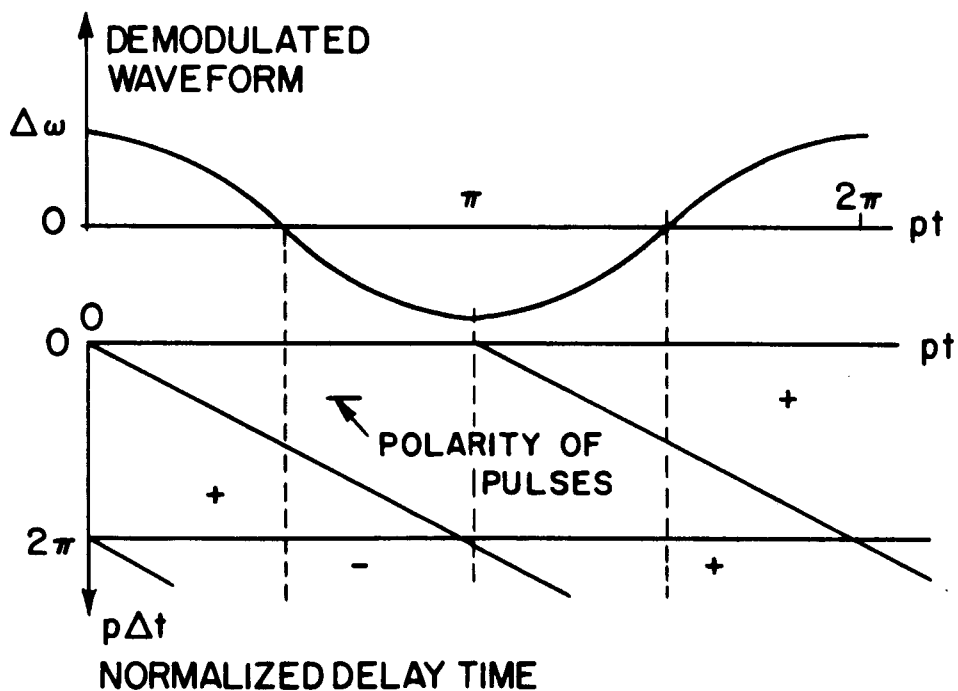
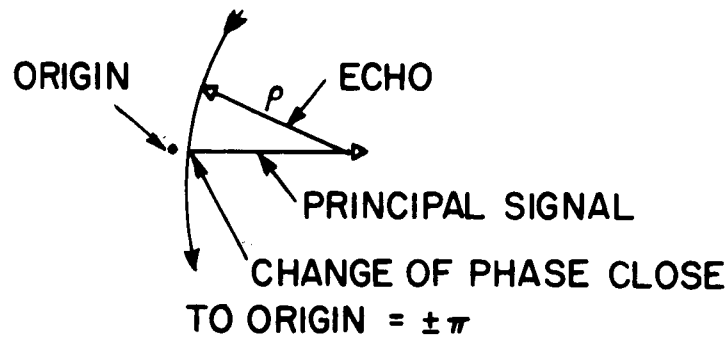
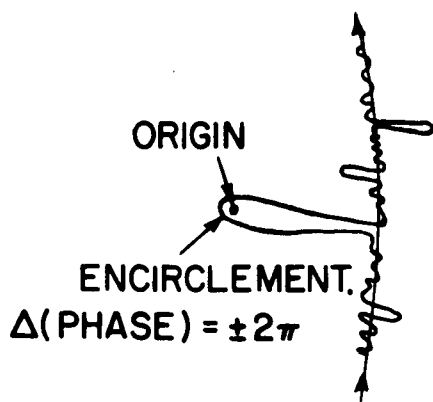
- 1) Waveform estimation - This includes optimum, real-time demodulators for FM or "twisted" modulation. The recursive approach ensures realizability as opposed to the "fixed observation" approach using Kashine-Loeve, integral equation techniques⁽³⁾. For example, the integral equation solution to maximum a-posteriori likelihood detectors requires many uncertain approximations and manipulations to extract a realizeable structure for the equations. This would not be the case of a recursive form of the solution can be found.
- 2) Adaptive Techniques - The use of recursive techniques reduces the complexity of the statistical description of the system (noise, signal, channel). Thus, if these are not known completely, a-priori, the measurement of this characteristics can be incorporated relatively simple into the receiver or processing structures. This will result in simultaneous measurement of channel parameters and processing of data.
- 3) Random channels and the effects of fading, multipath and other such disturbances can be incorporated into the model and studied. Diversity techniques can be handled as well.

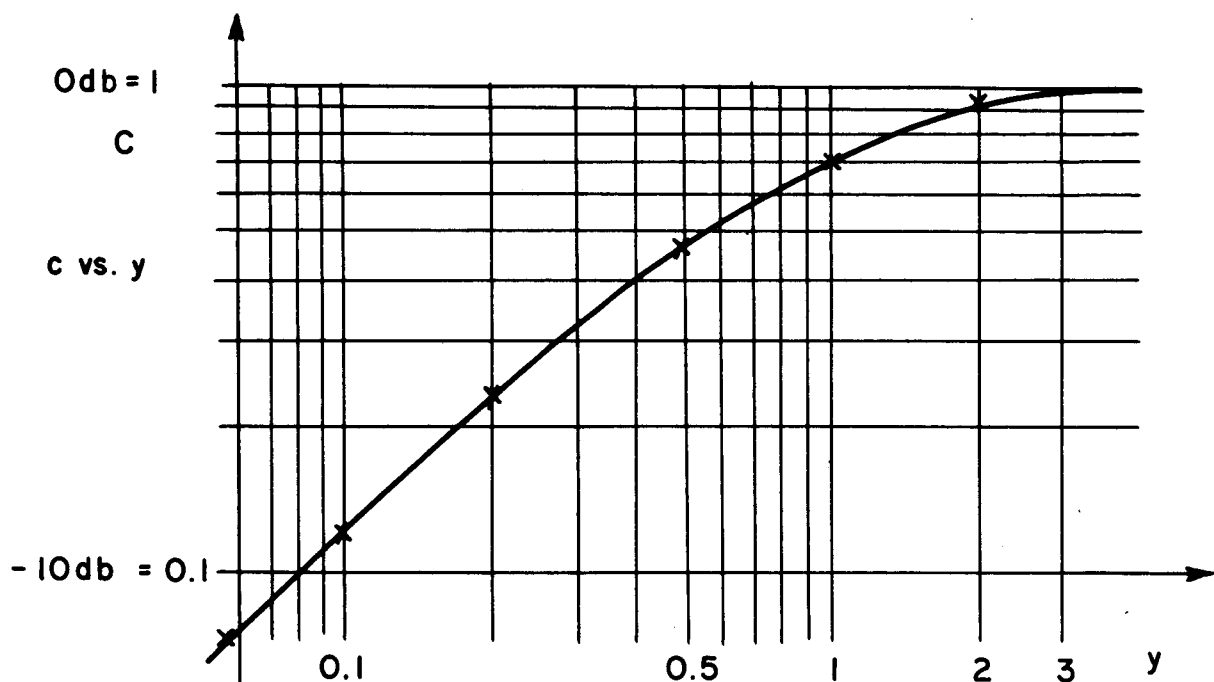
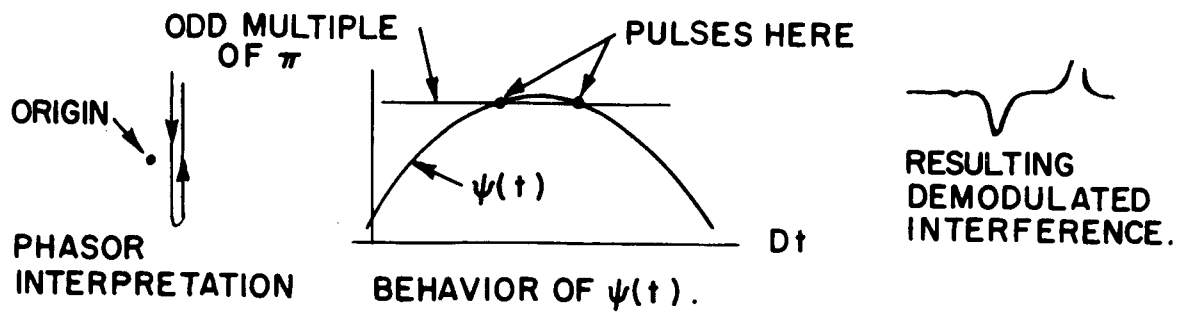
References

1. R.E. Kalman, "A New Approach to Linear Filtering and Prediction Problems" . ASME Trans., Vol. 820, March 1960.
2. Pickholtz, R. and Boorstyn, R., "A Recursive Approach to Signal Detection" to appear in IEEE Trans. on Information Theory, May 1968.
3. Van Trees, H.L., Detection, Estimation and Modulation Theory, John Wiley & Sons, 1968. Chapter 4.









$$C = 1 - \frac{1}{\pi} \int_0^{\frac{\pi}{2}} \sin^2 x e^{-\frac{y}{\sin x}} dx = \text{POWER GAIN OF INTERFERENCE IN FILTERS.}$$

